ACS APPLIED MATERIALS & INTERFACES

Letter

www.acsami.org

Flexible Light-Emitting Devices Based on Chirality-Sorted Semiconducting Carbon Nanotube Films

Dangmin Yu,[†] Huaping Liu,*[,‡,§] Lian-Mao Peng,[†] and Sheng Wang*[,†]

[†]Key Laboratory for the Physics and Chemistry of Nano Devices, Department of Electronics, Peking University, Beijing 100871, China

[‡]Beijing National Laboratory for Condensed Matter Physics, Institute of Physics, Chinese Academy of Sciences, Beijing 100190, China

[§]Collaborative Innovation Center of Quantum Matter, Beijing 100190, China

Supporting Information

ABSTRACT: Near-infrared light-emitting devices based on chirality-sorted (8,3), (8,4) enriched carbon nanotubes (CNTs) are fabricated on transparent and flexible substrate. The devices emit near-infrared light with well-defined wavelength, narrow peak width and high intensity. 500 times bending test also shows that the electric properties and electroluminescence (EL) spectra of devices do not decay apparently. This work demonstrates that chirality-sorted CNTs have large advantages in transparent and flexible infrared light source applications.

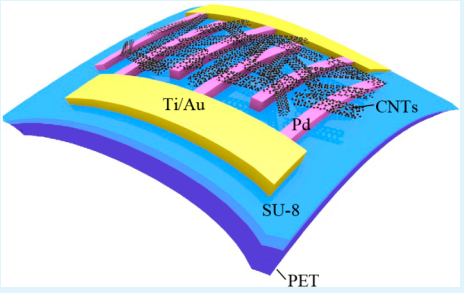

KEYWORDS: *carbon nanotube, infrared, electroluminescence, flexible, chirality sorted*

As application fields expand, flexible electronics and optoelectronics have attracted increasing attention. Examples include integrated circuit,[1] implantable medical devices,[2] sensors,[3] solar cells,[4] conformable radio frequency identification (RFID) tags,[5] touch screens,[6] displays,[7] and so on. Carbon nanotube (CNT) is a promising candidate for flexible devices because of its excellent electronic, optical, thermal and mechanical characteristics. Carbon nanotube has an intrinsic mobility greater than 100 000 $cm^2/(V\ s)$ at room temperature.[8] At the same time, semiconducting CNT is direct band gap 1D semiconductor, leading to the easier recombination of carriers than that in indirect band gap semiconductors. Infrared light-emitting devices have been fabricated based on CNTs using different kinds of samples and device sturctures.[9−12] Because the thermal conductivity of an individual single-walled CNT can be as high as 3500W/mK.[13] It helps devices sustain the heating generated by current. The mechanical property of CNT is also robust, for example, the Young's modulus of a CNT is about 1000 GPa,[14] which makes it stable to multitimes bending. All these advantages indicate the great potential of CNTs for flexible infrared light source and optoelectronic integrated system.

In early reports, CNT thin films, including network[15] and parallel array CNTs,[12] have been used as the channel materials to fabricate infrared light-emitting devices. Compared to single nanotube light-emitting devices, thin film devices fabricated by unsorted nanotubes are used to increase the luminous intensity through parallel connecting multiple CNTs and reducing the diversity between devices caused by different chirality. However, the previous CNT thin films used in light-emitting devices usually contained many kinds of chirality CNTs, leading to a broad emission spectrum. In practice, well-defined near-infrared wavelength and narrow peak width are important for application, especially in short distance transmission and control, such as the design of waveguides, modulators, and receivers.[16] Compared to the CNT thin film grown by chemical vapor method (CVD) directly, nanotubes separated by the gel chromatography method,[17] ultracentrifugation[18] and DNA wrapping chromatography[19] mainly contain one or two chiral CNTs. These chirality-sorted nanotubes have more advantages for infrared light source application. First, most of the metallic tubes have been removed after the separation processes, reducing the quenching of excitons with nonradiative energy transfer caused by metallic CNTs.[12,15] Second, chirality-sorted CNTs have selectable light-emitting wavelength determined by chirality and narrower peak width than that of CVD-grown CNTs containing many kinds of nanotubes. Third, exciton transfer between tubes in the chirality-sorted sample is relatively weaker than that in unsorted nanotube network films. Because only one or two main chiral CNTs limit the excitons of small diameter tubes decaying into the larger ones.[20]

In this letter, we present CNT light-emitting devices on flexible substrate using chirality-sorted (8,3), (8,4) CNT film as the channel material. As a result, spectrum of the CNT light source shows two well-defined peaks with narrow width,

Received: December 5, 2014
Accepted: February 5, 2015
Published: February 5, 2015

DOI: 10.1021/am508597c
ACS Appl. Mater. Interfaces 2015, 7, 3462−3467

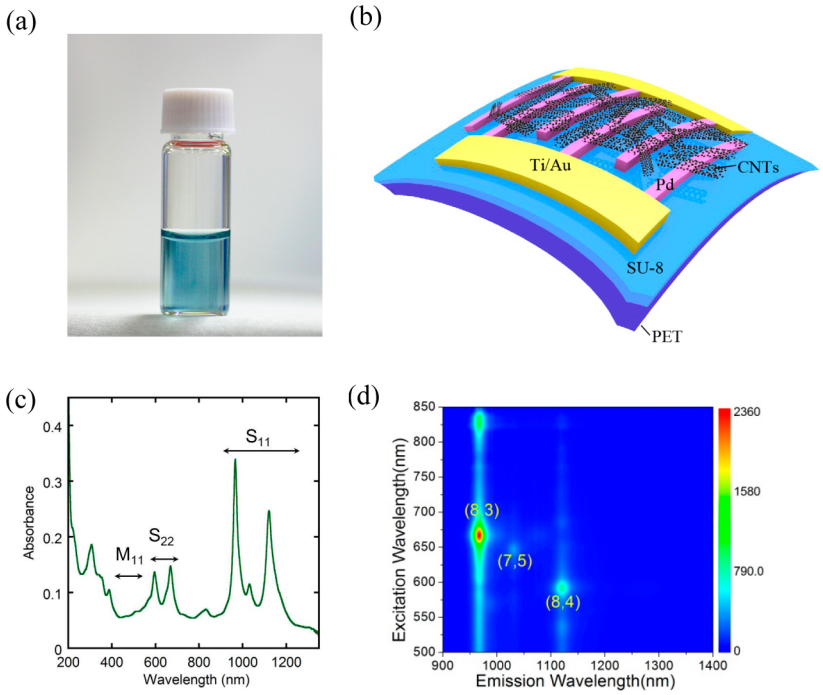

Figure 1. (a) (8,3), (8,4) chirality-enriched CNT solution prepared by gel chromatography method. (b) Structure of the CNT film light-emitting devices. The test pads are 5/45 nm Ti/Au (yellow) and the contact electrodes are 60 nm Pd (pink). The channel length and width of CNT film are 1 and 50 μm, respectively. The flexible substrate is constructed by PET covered by a layer of 50% SU-8 (2002) photoresist with thickness about 1 μm. (c) UV−vis−NIR absorption spectrum of the CNT sample. No obvious M_{11} peaks indicate the absence or very small amount of metallic CNTs. The S_{11} peaks located at 962, 1032, and 1119 nm are corresponding to (8,3), (7,5) and (8,4) CNTs, respectively. S_{22} peaks at 594 and 667 nm correspond to (8,3) and (8,4) CNTs, respectively. (d) Photoluminescence contour map of the sample. The characteristic peaks of (8,3) and (8,4) are at 968 and 1121 nm, respectively. There still exists small amount of (7,5) CNTs, corresponding to the emission wavelength at 1033 nm.

corresponding to the (8,3) and (8,4) CNTs, respectively. We also check the stability of flexible devices with bending test, and no obvious performance degradation is observed.

The chirality-sorted (8,3), (8,4) CNTs used in our experiment are sorted from HiPco nanotubes with gel chromatography method.[17] After the sorting process, CNTs are dispersed in 0.25% sodium deoxycholate (DOC) aqueous solution to avoid the formation of nanotube bundles (see Figure 1a). The (8,3) and (8,4) chirality-sorted semiconducting CNTs are used to fabricate the flexible light-emitting devices. Polyethylene terephthalate (PET) is chosen as the flexible substrate. Because the roughness of surface of PET used in this experiment is larger than 10 nm, it is not suitable to be the substrate for CNT thin film device fabrication. To obtain a smooth surface, 50% SU-8 (2002) photoresist, about 1 μm thickness, is spin-coated on the PET by 3000 r/min, and baked at 150 °C for 30 min. After the spin coating of SU-8 layer, root-mean-square (RMS) of the roughness of surface is only about 0.49 nm (see the Supporting Information, Figure S1), which is able to form flat nanotube films. Before fabricating the device electrodes, the substrate is modified by 3-triethoxysilylpropylamine (APTES) to increase the adhesion of CNTs. And then the substrate is immersed in the 2% APTES solution for 10 min, washed by IPA and dried by nitrogen blow. The device structure is patterned by electron-beam lithography (EBL) and a lift-off process. The contact electrodes are fabricated by 60 nm Palladium (Pd) and the test pads are 5/45 nm Titanium/Gold (Ti/Au). The channel length and width of the CNT film device is 1 and 50 μm, respectively. To obtain large enough injected current, four pairs of finger electrodes are used in a device as shown in Figure 1b. Then, chirality-sorted CNT solution is dropped onto the substrate directly and dried slowly. When the droplet is dry, the sample is washed with deionized water several times to remove the excess DOC to decrease the contact resistance between nanotubes and electrodes. After the EBL process, inductively coupled plasma (ICP) etching is used to remove the extra CNTs that are not in the channels. To keep the devices stable in the electroluminescence (EL) test, we spin-coated about 300 nm PMMA (50 K) on the sample.

Electrical measurements are carried out with a Keithley 4200 semiconductor analyzer at room temperature. Electroluminescence measurements are carried out with a 150 line/mm grating and a liquid-nitrogen-cooled InGaAs detector linear array of 512 × 1 pixels (detects E > 0.8 eV) (Jobin Yvon/Horiba Company). The spectra are collected using a microscope objective (50×) lens. The typical integration time for collecting an EL spectrum is 60 s. All measurements are performed in air.

To observe the morphology of the CNT film clearly, the solution was also dropped onto the Si/SiO_2 substrate and dried naturally. Typical CNT film is characterized by scanning electron microscope (SEM) image as shown in Figure S2 in the Supporting Information and the average CNT length is about 1 μm. Figure 1c shows the UV−vis−NIR absorption spectrum of the solution sample where are no obvious M_{11} peaks, indicating the absence or very small amount of metallic nanotubes. The S_{11} peaks at 962 nm (1.29 eV) and 1119 nm (1.11 eV) and S_{22} peaks at 594 nm (2.09 eV) and 667 nm (1.86 eV) correspond to (8,3) and (8,4) CNTs, respectively.[21] There also exists a small amount of (7,5) nanotubes in the sample, corresponding to the 1032 nm (1.20 eV) peak in the absorption spectrum. Figure 1d shows the photoluminescence (PL) contour map of

DOI: 10.1021/am508597c
ACS Appl. Mater. Interfaces 2015, 7, 3462−3467

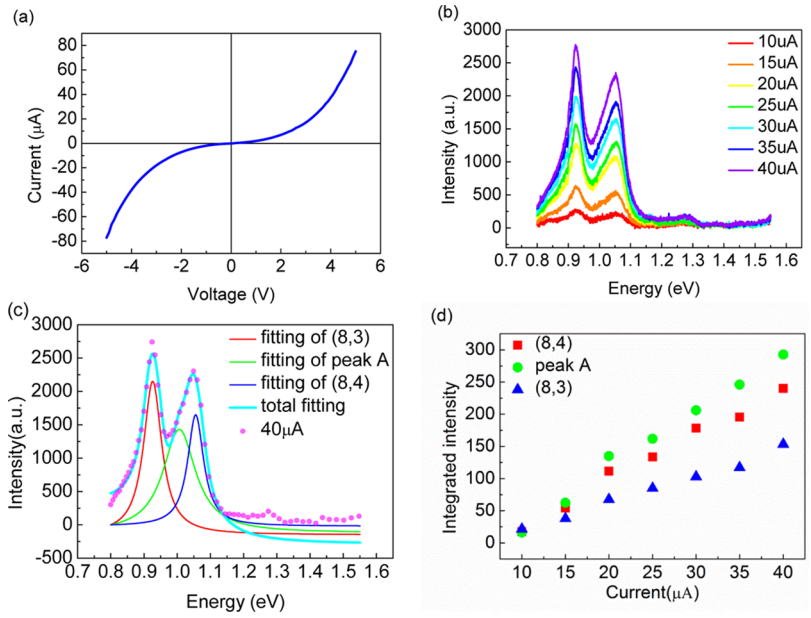

Figure 2. (a) Current−voltage curve of a typical device. (b) EL spectra of the device under different current. Two main EL peaks are corresponding to the (8,4) and (8,3) CNTs, respectively. (c) Lorentz fitting of the EL spectrum at current of 40 μA. The spectrum can be fitted by three peaks. (d) Integrated intensity of three peaks as a function of the current. All of them show a near linear relationship with the current.

CNT sample and the characteristic peaks of (8,3) and (8,4) are 968 nm (1.28 eV) and 1121 nm (1.11 eV), respectively. Raman spectra are also used to characterize the nanotube films with different wavelength lasers excitation (Figure S3a, b in the Supporting Information). Figure S3a in the Supporting Information shows the radial breath mode (RBM) peaks of (8,3) and (8,4) CNTs lying at 297 and 282 cm^{-1}, respectively. There are also some other RBM peaks in the spectra, which are the resonance peaks of other chirality CNTs, such as (9,7), (10,5), (11,3), (10,2), (9,1), and (10,3), excited by 785 and 633 nm lasers.[22] The D peak in Figure S3b in the Supporting Information shows that there are some defects in CNTs, which may be produced in dispersion process of nanotubes.

The current−voltage characteristic curve of a typical device is shown in Figure 2a and it indicates a complex transport mechanism in this film device. At small bias voltage, the few residual metallic CNTs contribute to most of the current due to large Schottky barrier (SB) existing between small diameter (<1 nm) semiconducting nanotubes and Pd electrodes. At large bias voltage, the semiconducting CNT channels turned on and supported majority of the current. It should be noted that CNTs with different chiralities are contacted to the electrodes in the thin film device, in which carriers have to overcome the tube−tube contacts to transport across the channel.

Figure 2b shows the EL spectra of the same device in Figure 2a. The threshold current and voltage for obvious EL spectrum is about 10 μA and 2.5 V, and the EL intensity increases with the increasing current from 10 to 40 μA. The spectra are dominated by two strong emission peaks at 0.93 and 1.06 eV, which may be assigned the two main chirality (8,4) and (8,3) nanotubes in the film, respectively. To further assign the EL peaks exactly to corresponding optical transitions of chirality nanotubes, one of the EL spectra (shown in Figure 2c) is fitted with three Lorentz lineshapes. The centers of three emission peaks are 0.93, 1.01, and 1.06 eV, respectively. The corresponding full width of half-maximum (fwhm) of three peaks is 66, 120, and 58 meV. In the spectra, the two strong EL peaks at 0.93 and 1.06 eV with relative narrower fwhm are attributed to E_{11} transitions of (8,4) and (8,3) CNTs, respectively. The PL spectra of the same CNT film on quartz substrate excited by 488 and 633 nm lasers are shown in Figure S4 (see the Supporting Information), in which the characteristic peaks of (8,4) and (8,3) are 1.07 and 1.26 eV, respectively, about 0.02 eV red shift compared to the PL peaks of CNT sample in solution shown in Figure 1d. There still exists the peak of (7,5) CNTs in the PL spectrum. Because the 633 nm laser is close to the resonance E_{22} energy of (7,5) CNT at 645 nm, which causes the relatively strong emission peak of the (7,5) CNT in the PL spectrum. The EL peaks of (8,4) and (8,3) are about 140 and 200 meV redshift compared to PL of CNT film, respectively. The redshift is not an accidental phenomenon and the statistical result of 15 devices fabricated in one batch shows almost constant results (see the Supporting Information, Figure S5). The redshift cannot be simply attributed to the exciton transformation from (8,3) or (8,4) nanotubes to larger diameter ones. First, the amount of other kinds of CNTs is limited. Second, if the exciton transformation dominates the EL process, the spectra should show a broad peak at the lowest energy region. However, there are two narrower peaks with a weaker peak sandwiched in them, meaning that the excitons transfer neither to the lowest energy state nor the adjacent energy state, which is unreasonable. Possible reasons for redshift of the EL spectra may be the bundle of nanotubes,[23] localized excitons at structural defect sites,[10] drain-field-induced doping that leads to enhanced dielectric screening[24] and so on. In such solution processed samples, the defects related intrinsic dark state may lead to a large EL redshift.[10,20] The drain induced doping leads to spectra redshift due to the increasing screening of Coulomb interaction in the CNT with the high doping level which are responsible for both a renormalization of the band gap and a reduction of the exciton binding energy.[24] While the result based on ab initio calculation and effective mass (EM) approach shows that doping causes the reduction of band

DOI: 10.1021/am508597c
ACS Appl. Mater. Interfaces 2015, 7, 3462−3467

gaps and exciton binding energies, leading to a blueshift.[25] Whether the spectral redshift are attributable to doping is still controversial. The reasons of large redshift in our experiment need further investigation.

In the EL spectra (Figure 2c), the peak at 1.01 eV (peak A) was wider than the other two peaks. It can be assigned to the following transitions: (a) the existence of a small amount of (7,5) CNTs whose E_{11} peak lies between (8,4) and (8,3) CNTs. From the absorption and the PL spectra, there is an obvious (7,5) nanotube characteristic peak. (b) EL emission from the local defects of (8,3) CNTs. The dispersion process introduced defects to the sample inevitably, which is confirmed by the D peak in the Raman spectrum (Figure S3b in the Supporting Information). As defect energy levels usually lie lower than the E_{11} energy level, leading to an extra peak at lower energy region relative to the intrinsic EL peaks. (c) Exciton transfer from (8,3) nanotubes to (7,5) nanotubes in the films. On the one hand, the migration of nanotubes during the drying process of the samples may generate more bundles, which may provide a pathway for exciton transfer between nanotubes. On the other hand, the CNT solution is high concentration, leading to a high density of CNTs on substrate after drying. Both make it possible for some exciton transfer between nanotubes in the sample.[26] At large current, EL peaks at 1.27 eV begin to appear and it may correspond to the interband transition of (8,3) nanotubes at local strong electric field.

To explore the EL mechanism of the chirality sorted CNT films, the intensity−current relationship is shown in Figure 2d. Both (8,4) and (8,3) characteristic peaks show a near-linear relationship with the current, which is in accordance with the characteristics of ambipolar radiation recombination under low electric field of 2−3 V/μm. Although the device is fabricated using symmetrical Pd contact electrodes, the existing SB barriers both for electron and hole injection in the thin film may lead to ambipolar recombination.[24,27] Because of the average length of nanotubes about 1 μm and the curving morphology, carriers may transit more than two CNTs from one electrode to the other and go through at least one tube−tube junction for the 1 μm channel length. Therefore, electrons and holes may have different transport pathways in the thin film, and then form excitons and recombine radiatively.[27]

For most near-infrared light source applications, including chemical spectroscopy and sensing,[28] optical fiber communication,[29] and on-chip optoelectronic integrated circuits, a nearly monochromatic light is needed. Because the EL peak positions are mainly determined by chirality of the CNTs. For various applications, different chirality CNTs can be chosen to obtain a certain EL wavelength.[17−19] For example, the 0.93 eV light emitted by (8,4) chirality CNT is close to the 1330 nm communication wavelength. The peak width about dozens of meV is narrow enough to meet the requirement of most applications, like optical communications. More importantly, both centers of the two EL peaks keep stable with the increasing current (Figure 3a) and there is only small fluctuation of the three peaks' width (Figure 3b). The phenomenon also supports that no obvious change of proposed EL mechanism within the current or voltage range.

To confirm the stability of devices during folding process, we compared the electric and EL characteristics of a device before and after bending test for 500 times in Figure 4. Typical bending test is shown in Figure 4a and the bending radius is about 2−3 mm. Figure 4b shows the current−voltage curves of

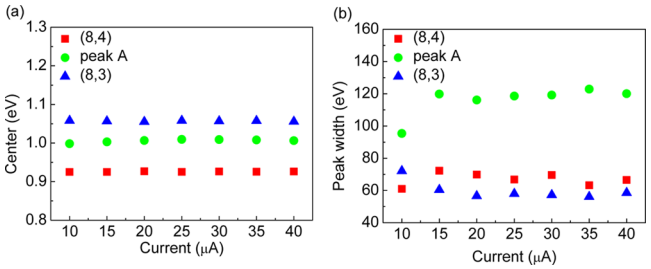

Figure 3. (a) Center of EL three peaks dependent on the current. All of them keep stable with the increasing current. (b) Width of three peaks change with the increasing current.

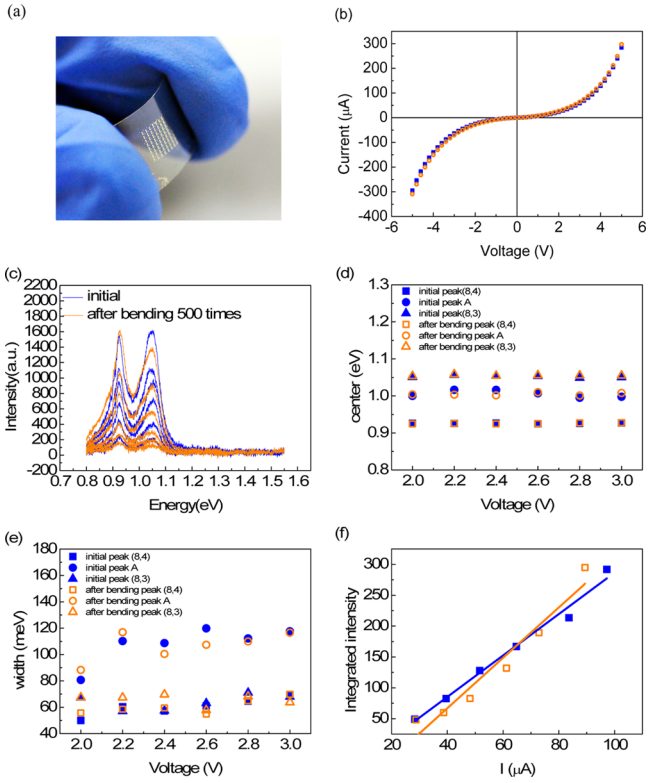

Figure 4. Comparison of the device performance before and after bending test for 500 times with the bending radius about 2−3 mm. Blue and orange curves represent the original state and after-bending, respectively. (a) Photo of the bending sample. (b) Electric property of the device. The *I*−*V* curves almost coincided with each other before and after bending test. (c) EL spectra of the device at different current. (d) Center of the peaks variety with the voltage show that all of three peaks center are unchanged. (e) Width of the peaks dependent on the voltage. (f) Relationship between total integrated intensity and the current of the device before and after bending test.

the device before (blue) and after (orange) bending test. They are almost coincided with each other, indicating that the CNTs in channel are not broken down under such a process. This is attributed to the excellent mechanical property of CNTs and the network structure of CNT films. To verify the EL property of the device, the spectra are obtained under the same measurement condition before and after bending test. As Figure 4c−e shows, the characteristics of the EL spectra basically maintained. At the same time, the positions of all three peaks stay unchanged, suggesting that the fold process does not obviously change the intrinsic EL property of the device. Figure 4f shows the relationship of total integrated intensity with

DOI: 10.1021/am508597c
ACS Appl. Mater. Interfaces 2015, 7, 3462−3467

current. The slope reflects the radiation efficiency of devices, and it appears there is no obvious change before and after the bending test. The top and bottom surfaces of the chirality-sorted nanotubes are organic PMMA (50K) and SU-8, decreasing the nonradiative recombination commonly happened for nanotubes on Si/SiO_2 substrate.[30] A total of 25 devices are tested with the same process, and 100% of them still work after the bending test is performed 500 times.

In summary, we have demonstrated the infrared light-emitting devices based on chirality-sorted (8,3), (8,4) CNTs thin film on PET substrate for flexible and transparent optoelectronics. The EL spectra of nanotube devices show two main characteristic peaks corresponding to (8,3) and (8,4) chirality-enriched CNT and narrow peak widths several tens of milli-electron volts. After the bending test is performed 500 times, the electric and EL performance of devices is still good and the result statistics show that all of 25 devices still work. The excellent electrical, optical, thermal, and mechanical properties of chirality-sorted CNTs make it competent in transparent and flexible infrared light-emitting source applications.

■ ASSOCIATED CONTENT

Supporting Information

Figure S1 shows the AFM photograph of the SU-8 surface. Figure S2 shows the SEM image of CNT film. Figure S3 shows the Raman spectra of the chirality-sorted CNT sample. Figure S4 shows the PL spectra of the same (8,3), (8,4) CNT film on substrate excited by 488 and 633 nm lasers. Figure S5 shows the statistical result of the peak position of 15 devices fabricated in one batch. This material is available free of charge via the Internet at http://pubs.acs.org.

■ AUTHOR INFORMATION

Corresponding Authors

*E-mail: shengwang@pku.edu.cn.
*E-mail: liuhuaping@iphy.ac.cn.

Notes

The authors declare no competing financial interest.

■ ACKNOWLEDGMENTS

We thank Haitao Xu, Yiran Liang, Fanglin Wang, Yang Liu, Nan Wei, Ze Ma, and Hua Zhong for helpful discussions. This work was supported by the Ministry of Science and Technology of China (Grants 2011CB933001 and 2011CB933002), National Science Foundation of China (Grants 61370009, 61271051, 61321001), and Beijing Municipal Science and Technology Commission (Grants Z131100003213021 and 20121000102). H.L. acknowledges support by the recruitment program of global youth experts and the "100 talents project" of CAS.

■ REFERENCES

(1) Cao, Q.; Kim, H.-S.; Pimparkar, N.; Kulkarni, J. P.; Wang, C.; Shim, M.; Roy, K.; Alam, M. A.; Rogers, J. A. Medium-scale Carbon Nanotube Thin-film Integrated Circuits on Flexible Plastic Substrates. *Nature* **2008**, *454*, 495−500.

(2) Kim, D.-H.; Viventi, J.; Amsden, J. J.; Xiao, J.; Vigeland, L.; Kim, Y.-S.; Blanco, J. A.; Panilaitis, B.; Frechette, E. S.; Contreras, D.; Kaplan, D. L.; Omenetto, F. G.; Huang, Y.; Hwang, K.-C.; Zakin, M. R.; Litt, B.; Rogers, J. A. Dissolvable Films of Silk Fbroin for Ultrathin Conformal Bio-integrated Electronics. *Nat. Mater.* **2010**, *9*, 511−517.

(3) Takahashi, T.; Takei, K.; Gillies, A. G.; Fearing, R. S.; Javey, A. Carbon Nanotube Active-Matrix Backplanes for Conformal Electronics and Sensors. *Nano Lett.* **2011**, *11*, 5408−5413.

(4) Lipomi, D. J.; Tee, B. C. K.; Vosgueritchian, M.; Bao, Z. Stretchable Organic Solar Cells. *Adv. Mater.* **2011**, *23*, 1771−1775.

(5) Jung, M.; Kim, J.; Noh, J.; Lim, N.; Lim, C.; Lee, G.; Kim, J.; Kang, H.; Jung, K.; Leonard, A. D.; Tour, J. M.; Cho, G. All Printed and Roll-to-roll Printable 13.56 MHz Operated 1-bit RF Tag on Plastic Foils. *IEEE Trans. Electron Dev.* **2010**, *57*, 571−580.

(6) Bae, S.; Kim, H.; Lee, Y.; Xu, X.; Park, J.-S.; Zheng, Y.; Balakrishnan, J.; Lei, T.; Kim, H. Ri; Song, Y. I.; Kim, Y.-J.; Kim, K. S.; Ozyilmaz, B.; Ahn, J.-H.; Hong, B. H.; Iijima, S. Roll-to-roll Production of 30-in. Graphene Films for Transparent Electrodes. *Nat. Nanotechnol.* **2010**, *5*, 574−578.

(7) Gelinck, G. H.; Huitema, H. E. A.; van Veenendaal, E.; Cantatore, E.; Schrijnemakers, L.; van der Putten, J. B. P. H.; Geuns, T. C. T.; Beenhakkers, M.; Giesbers, J. B.; Huisman, B.-H.; Meijer, E. J.; Benito, E. M.; Touwslager, F. J.; Marsman, A. W.; van Rens, B. J. E.; de Leeuw, D. M. Flexible Active-matrix Displays and Shift Registers Based on Solution-processed Organic Transistors. *Nat. Mater.* **2004**, *3*, 106−110.

(8) Durkop, T.; Getty, S. A.; Cobas, E.; Fuhrer, M. S. Extraordinary Mobility in Semiconducting Carbon Nanotubes. *Nano Lett.* **2004**, *4*, 35−39.

(9) Misewich, J. A.; Martel, R.; Avouris, P.; Tsang, J. C.; Heinze, S.; Tersoff, J. Electrically Induced Optical Emission from a Carbon Nanotube FET. *Science* **2003**, *300*, 783−786.

(10) Wang, S.; Zeng, Q. S.; Yang, L. J.; Zhang, Z. Y.; Wang, Z. X.; Pei, T.; Ding, L.; Liang, X. L.; Gao, M.; Li, Y.; Peng, L. M. High-Performance Carbon Nanotube Light-Emitting Diodes with Asymmetric Contacts. *Nano Lett.* **2011**, *11*, 23−29.

(11) Yu, D.; Wang, S.; Ye, L.; Li, W.; Zhang, Z.; Chen, Y.; Zhang, J.; Peng, L. M. Electroluminescence from Serpentine Carbon Nanotube Based Light-Emitting Diodes on Quartz. *Small* **2013**, *10*, 1050−1056.

(12) Kinoshita, M.; Steiner, M.; Engel, M.; Small, J. P.; Green, A. A.; Hersam, M. C.; Krupke, R.; Mendez, E. E.; Avouris, P. The Polarized Carbon Nanotube Thin Film LED. *Opt. Express* **2010**, *18*, 25738−25745.

(13) Pop, E.; Mann, David.; Wang, Q.; Goodson, K.; Dai, H. Thermal Conductance of an Individual Single-Wall Carbon Nanotube above Room Temperature. *Nano Lett.* **2006**, *6*, 96−100.

(14) Treacy, M. M. J.; Ebbesen, T. W.; Gibson, J. M. Exceptionally High Young's Modulus Observed for Individual Carbon Nanotubes. *Nature* **1996**, *381*, 678−680.

(15) Adam, E.; Aguirre, C. M.; Marty, L.; St-Antoine, B. C.; Meunier, F.; Desjardins, P.; Ménard, D.; Martel, R. Electroluminescence from Single-wall Carbon Nanotube Network Transistors. *Nano Lett.* **2008**, *8*, 2351−2355.

(16) Sorger, V. J.; Oulton, R. F.; Ma, R.-M.; Zhang, X. Toward Integrated Plasmonic Circuits. *MRS Bull.* **2012**, *37*, 728−738.

(17) Liu, H. P.; Nishide, D.; Tanaka, T.; Kataura, H. Large-scale Single-chirality Separation of Single-wall Carbon Nanotubes by Simple Gel Chromatography. *Nat. Commun.* **2011**, *2*, 309.

(18) Arnold, M. S.; Green, A. A.; Hulvat, J. F.; Stupp, S. I.; Hersam, M. C. Sorting Carbon Nanotubes by Electronic Structure Using Density Differentiation. *Nat. Nanotechnol.* **2006**, *1*, 60−65.

(19) Zheng, M.; Jagota, A.; Strano, M. S.; Santos, A. P.; Barone, P.; Chou, S. G.; Diner, B. A.; Dresselhaus, M. S.; Mclean, R. S.; Onoa, G. B.; Samsonidze, G. G.; Semke, E.; Usrey, D. M.; Walls, D. J. Structure-based Carbon Nanotube Sorting by Sequence-dependent DNA Assembly. *Science* **2003**, *302*, 1545−1548.

(20) Engel, M.; Small, J. P.; Steiner, M.; Freitag, M.; Green, A. A.; Hersam, M. C.; Avouris, P. Thin Film Nanotube Transistors Based on Self-assembled, Aligned, Semiconducting Carbon Nanotube Arrays. *ACS Nano* **2008**, *2*, 12.

(21) Weisman, R. B.; Bachilo, S. M. Dependence of Optical Transition Energies on Structure for Single-Walled Carbon Nanotubes in Aqueous Suspension: An Empirical Kataura Plot. *Nano Lett.* **2003**, *3*, 1235−1238.

DOI: 10.1021/am508597c
ACS Appl. Mater. Interfaces 2015, 7, 3462−3467

(22) Bachilo, S. M.; Strano, M. S.; Kittrell, C.; Hauge, R. H.; Smalley, R. E.; Weisman, R. B. Structure-assigned Optical Spectra of Single-walled Carbon Nanotubes. *Science* **2002**, *298*, 2361−2366.
(23) Reich, S.; Thomsen, C. Electronic Band Structure of Isolated and Bundled Carbon Nanotubes. *Phys. Rev. B* **2002**, *65*, 155411.
(24) Freitag, M.; Steiner, M.; Naumov, A.; Avouris, P. Carbon Nanotube Photo- and Electroluminescence in Longitudinal Electric Fields. *ACS Nano* **2009**, *3*, 3744−3748.
(25) Spataru, C. D.; Leonard, F. Tunable Band Gaps and Excitons in Doped Semiconducting Carbon Nanotubes Made Possible by Acoustic Plasmons. *Phys. Rev. Lett.* **2010**, *104*, 177402.
(26) Grechko, M.; Ye, Y.; Mehlenbacher, R. D.; McDonough, T. J.; Wu, M.; Jacobberger, R. M.; Arnold, M. S.; Zanni, M. T. Diffusion-Assisted Photoexcitation Transfer in Coupled Semiconducting Carbon Nanotube Thin Films. *ACS Nano* **2014**, *8*, 5383−5394.
(27) Jakubka, F.; Backes, C.; Gannott, F.; Mundloch, U.; Hauke, F.; Hirsch, A.; Zaumseil, J. Mapping Charge Transport by Electroluminescence in Chirality-Selected Carbon Nanotube Networks. *ACS Nano* **2013**, *7*, 7428−7435.
(28) Siesler, H. W.; Ozaki, Y.; Kawata, S.; Heise, H. M. *Near-Infrared Spectroscopy: Principles, Instruments, Applications*; Wiley−VCH: Weinheim, Germany, 2002.
(29) Kazovsky, L. G.; Benedetto, S.; Willner, A. E. *Optical Fiber Communication Systems*; Artech House: Norwood, MA, 1996.
(30) Ai, N.; Walden-Newman, W.; Song, Q.; Kalliakos, S.; Strauf, S. Suppression of Blinking and Enhanced Exciton Emission from Individual Carbon Nanotubes. *ACS Nano* **2011**, *5*, 2664−2670.

DOI: 10.1021/am508597c
ACS Appl. Mater. Interfaces 2015, 7, 3462−3467